Journal of Medicinal Chemistry

Article

pubs.acs.org/jmc

Discovery of a Potent Stapled Helix Peptide That Binds to the 70N Domain of Replication Protein A

Andreas O. Frank,[†,‡,#] Bhavatarini Vangamudi,[†,∞] Michael D. Feldkamp,[†,‡] Elaine M. Souza-Fagundes,[†,¶] Jessica W. Luzwick,[†] David Cortez,[†] Edward T. Olejniczak,[†,‡] Alex G. Waterson,[§,∥] Olivia W. Rossanese,[†] Walter J. Chazin,[†,‡,§,∥] and Stephen W. Fesik*[,†,‡,§,∥]

[†]Department of Biochemistry, Vanderbilt University School of Medicine, Nashville, Tennessee 37232-0146, United States

[‡]Center for Structural Biology, Vanderbilt University, Nashville, Tennessee 37232-8725, United States

[§]Department of Pharmacology, Vanderbilt University School of Medicine, Nashville, Tennessee 37232-6600, United States

[∥]Department of Chemistry, Vanderbilt University, Nashville, Tennessee 37232-1822, United States

Supporting Information

ABSTRACT: Stapled helix peptides can serve as useful tools for inhibiting protein−protein interactions but can be difficult to optimize for affinity. Here we describe the discovery and optimization of a stapled helix peptide that binds to the N-terminal domain of the 70 kDa subunit of replication protein A (RPA70N). In addition to applying traditional optimization strategies, we employed a novel approach for efficiently designing peptides containing unnatural amino acids. We discovered hot spots in the target protein using a fragment-based screen, identified the amino acid that binds to the hot spot, and selected an unnatural amino acid to incorporate, based on the structure−activity relationships of small molecules that bind to this site. The resulting stapled helix peptide potently and selectively binds to RPA70N, does not disrupt ssDNA binding, and penetrates cells. This peptide may serve as a probe to explore the therapeutic potential of RPA70N inhibition in cancer.

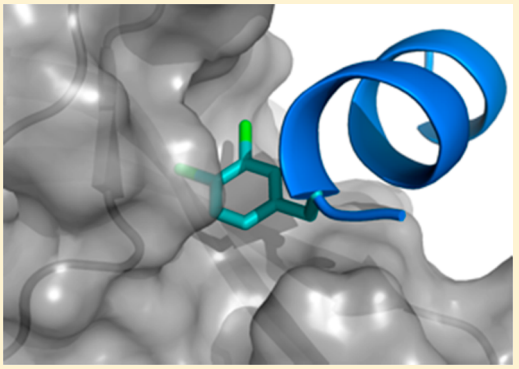

INTRODUCTION

Replication protein A (RPA) is a single stranded DNA (ssDNA)−binding protein complex that is essential for DNA replication, damage response, and repair.[1,2] In response to DNA lesion formation, RPA rapidly coats ssDNA,[1,3] preventing the formation of aberrant DNA structures at replication foci and recruiting a number of checkpoint proteins to initiate the response to DNA damage.[4] Increased activity of DNA damage response and repair pathways is observed in a number of human cancers and has been linked to resistance to radiation or chemotherapy treatment.[5] Thus, compounds targeting these pathways may have utility in patients undergoing cancer therapy.

RPA70 is the largest of the RPA subunits and contains three high-affinity ssDNA binding domains that serve as the DNA-anchoring core of the entire complex (RPA70A, -B, -C).[1,2] Binding to ssDNA is mediated by oligosaccharide/oligonucleotide binding (OB) folds that are present on all subunits.[6−8] The basic cleft in the OB fold present on the N-terminal domain, RPA70N, binds to several partner proteins that are important for mediating the response to DNA damage, including ATRIP (ATR-interacting protein), RAD9, MRE11, and p53.[4,9−11] We hypothesize that the selective inhibition of the RPA70N basic cleft will specifically disrupt these protein−protein interactions, leading to the inhibition of a subset of RPA functions, attenuation of the DNA damage response, and the selective killing of cancer cells.

Toward the discovery of a probe molecule that binds tightly to RPA70N and inhibits its interaction with other proteins, we and others have previously reported small molecules that bind to RPA70N.[12−14] We used an NMR-based screen to identify fragments that bind to RPA70N, and, on the basis of X-ray structures of the screening hits and analogues when bound to the protein, have obtained analogues with improved affinity. Recently, we have discovered compounds that bind to RPA70N with submicromolar affinity[12] that were obtained by linking together small molecules that bind to two adjacent sites.

An alternative approach for targeting protein−protein interactions is the use of stapled helix peptides. Hydrocarbon stapling has been shown to increase the affinity, stability, and cellular permeability of peptide sequences that bind to protein targets.[15−17] NMR experiments have demonstrated that homologous peptides derived from the partner proteins ATRIP, RAD9, and MRE11 bind competitively to the basic cleft of RPA70N.[18] Further, the three peptides share a region of similar primary sequence with p53 and contain a mix of conserved acidic and hydrophobic amino acid residues.[19] An X-

Received: November 11, 2013
Published: February 3, 2014

   dx.doi.org/10.1021/jm401730y | J. Med. Chem. 2014, 57, 2455−2461

ray crystal structure of a chimeric protein containing portions of RPA70N and p53 reveals that a part of the p53 transactivation domain (residues 47−57) folds into helices that bind into the basic cleft in the OB fold of RPA70N.[19] These binding interactions in the cleft are stabilized by both electrostatic and hydrophobic interactions. We have previously measured the binding affinity of these peptides to RPA70N and found that the ATRIP-derived sequence binds more tightly than the Rad9, MRE11, and p53 peptides.[20]

Here we describe the discovery of stapled helix peptides, based on the ATRIP sequence, that bind tightly to the protein−protein interaction site in the basic cleft of RPA70N and inhibit the interactions of RPA70N with other peptides/proteins. The binding affinity was optimized by traditional methods, as well as a novel method that can efficiently select and incorporate unnatural amino acids into the peptides. Peptides in which an unnatural amino acid was incorporated displayed a 1−2 orders of magnitude improvement in binding affinity compared to peptides with natural amino acids, penetrate cells, and may serve as useful tools for studying RPA function and the therapeutic potential of inhibiting RPA.

RESULTS AND DISCUSSION

Alanine Scanning of the ATRIP Peptide. To better understand the peptide structure−activity-relationships (SARs) of the ATRIP-derived peptide and to elucidate the sequence positions suitable for affinity-optimizing point mutations, we performed an alanine scan in which each amino acid was replaced by an alanine residue (Table 1). Affinity of the mutated peptides was measured using an FPA competition assay with FITC-ATRIP as a probe.[20]

Residues D1, F2, T3, D6, L7, E9, L10, D11, and L13 were found to be important for binding to RPA70N, as replacement of each of these with an alanine resulted in a significant loss of binding affinity. Interestingly, although D5 is conserved in the ATRIP and corresponding RAD9, MRE11, and p53 sequences, replacement with an alanine leads to a peptide equipotent with the parent, suggesting that this residue does not contribute significantly to binding to RPA70N. Similarly, despite the conservation of E8 in three out of the four RPA70N binding partners, no loss of binding was observed when E8 was replaced with alanine. In contrast, an almost complete loss of binding was observed when F2 was replaced with an alanine (peptide-02). Two ATRIP amino acid mutations led to a slight improvement in affinity: E8A (peptide-07, K_d = 22 μM) and T12A (peptide-11, K_d = 17 μM). However, when combined into one peptide sequence (peptide-14), the individual positive effects on the binding affinity were not additive.

Table 1. Alanine Scan of an ATRIP-Derived Peptide

Peptide Name	Amino Acid Sequence[a]	FPA K_d (μM)[b]
ATRIP	Ac-DFTADDLEELDTLAS-NH_2	29 ± 3[c]
Peptide-01	Ac-**A**FTADDLEELDTLAS-NH_2	152 ± 36
Peptide-02	Ac-D**A**TADDLEELDTLAS-NH_2	>1000
Peptide-03	Ac-DF**A**ADDLEELDTLAS-NH_2	152 ± 28
Peptide-04	Ac-DFTA**A**DLEELDTLAS-NH_2	31 ± 9
Peptide-05	Ac-DFTAD**A**LEELDTLAS-NH_2	225 ± 27
Peptide-06	Ac-DFTADD**A**EELDTLAS-NH_2	172 ± 20
Peptide-07	Ac-DFTADDL**A**ELDTLAS-NH_2	22 ± 4
Peptide-08	Ac-DFTADDLE**A**LDTLAS-NH_2	167 ± 26
Peptide-09	Ac-DFTADDLEE**A**DTLAS-NH_2	197 ± 25
Peptide-10	Ac-DFTADDLEEL**A**TLAS-NH_2	85 ± 15
Peptide-11	Ac-DFTADDLEELD**A**LAS-NH_2	17 ± 1
Peptide-12	Ac-DFTADDLEELDT**A**AS-NH_2	63 ± 15
Peptide-13	Ac-DFTADDLEELDTLA**A**-NH_2	26 ± 7
Peptide-14	Ac-DFTADDL**A**ELD**A**LAS-NH_2	20 ± 5

[a]Alanine mutations are shown in bold red. [b]K_d values derived from IC_{50} values measured in an FPA competition assay. [c]Souza-Fagundes et al.[20]

ATRIP Amino Acid Substitutions Inspired by p53. In an attempt to improve the binding affinity of the ATRIP peptide, we substituted the hydrophobic residues WF from the p53 peptide into the corresponding positions of the ATRIP peptide (Table 2). These residues form a hydrophobic motif within p53 (IEQWF) that is not present within the ATRIP sequence. Although individual substitution of L10 or D11 with W or F, respectively, did not improve binding relative to peptide-14 (peptide-15 and peptide-16), a 10-fold improvement in affinity was observed when these replacements were combined (peptide-17, K_d = 2.7 μM). This effect may be attributed to a clustering of the two residues, leading to the formation of a hydrophobic binding core.[19,21] To further optimize the potency, we substituted positions 8 and 12 of peptide-17 with alanines, as those mutations were found to increase the binding affinity to RPA70N. Whereas the E8A mutation results in a dramatic loss of affinity in the context of the WF motif (peptide-18), the binding of peptide-19 (T12A mutation) was increased by a factor of 2 relative to peptide 17. A FITC moiety was attached to peptide-19 to facilitate direct measurement of binding affinity to RPA70N; the new peptide-20 has an affinity of 480 nM (approximately an additional 3-fold increase). While the basis for the binding improvement due to the FITC label is not well understood, a similar effect was noted with the ATRIP peptide.[20]

Table 2. Amino Acid Substitutions

Peptide Name	Amino Acid Sequence[a]	FPA K_d (μM)[b]
p53	Ac-MLSPDDIEQWFTEDP-NH_2	100 ± 8[c]
ATRIP	Ac-DFTADDLEELDTLAS-NH_2	29 ± 3[c]
FITC-ATRIP	FITC-DFTADDLEELDTLAS-NH_2	6.4 ± 1.1[c,d]
Peptide-15	Ac-DFTADDLEEL**F**TLAS-NH_2	22 ± 1
Peptide-16	Ac-DFTADDLEE**W**DTLAS-NH_2	138 ± 6
Peptide-17	Ac-DFTADDLEE**WF**TLAS-NH_2	2.7 ± 0.3
Peptide-18	Ac-DFTADDL**A**E**WF**TLAS-NH_2	43 ± 4
Peptide-19	Ac-DFTADDLEE**WFA**LAS-NH_2	1.2 ± 0.1
Peptide-20	FITC-DFTADDLEE**WFA**LAS-NH_2	0.48 ± 0.03[d]

[a]Substituted residues are indicated in bold red. [b]K_d values derived from IC_{50} values measured in an FPA competition assay. [c]Souza-Fagundes et al.[20] [d]K_d values of FITC-labeled peptides determined by direct binding experiments.

Reduction of Overall Peptide Charge. Peptide-20 has a net negative charge of −6. Empirical evidence has suggested

dx.doi.org/10.1021/jm401730y | J. Med. Chem. 2014, 57, 2455−2461

that a neutral or positive overall charge is optimal for achieving cellular penetrance.[17] We therefore examined the relative importance of the negatively charged residues in peptide-19 by replacing aspartic and glutamic acid residues with their amide analogues. In addition, we tested the replacement of D and E residues with alanines (in the context of the optimized WFA containing peptide-19) to elucidate which negatively charged amino acids could be substituted with an uncharged residue without leading to an unacceptable decrease in RPA70N affinity (Table 3). While replacement of some

Table 3. Charge Abrogation of Peptide-19

Peptide Name	Amino Acid Sequence[a]	FPA K_d (μM)[b]	Net Charge
Peptide-19	Ac-DFTADDLEEWFALAS-NH_2	1.2 ± 0.1	-5
Peptide-20	FITC-DFTADDLEEWFALAS-NH_2	0.48 ± 0.03[c]	-6
Peptide-21	Ac-**N**FTADDLEEWFALAS-NH_2	5.8 ± 1.1	-4
Peptide-22	Ac-DFTA**A**DLEEWFALAS-NH_2	2.3 ± 1.1	-4
Peptide-23	Ac-DFTA**N**DLEEWFALAS-NH_2	19 ± 8	-4
Peptide-24	Ac-DFTAD**A**LEEWFALAS-NH_2	28 ± 4	-4
Peptide-25	Ac-DFTAD**N**LEEWFALAS-NH_2	6.9 ± 3.0	-4
Peptide-26	Ac-DFTADDL**A**EWFALAS-NH_2	28 ± 5	-4
Peptide-27	Ac-DFTADDLE**A**WFALAS-NH_2	2.4 ± 0.4	-4
Peptide-28	Ac-DFTADDLE**Q**WFALAS-NH_2	2.6 ± 0.4	-4
Peptide-29	FITC-**N**FTA**AN**LE**A**WFALAS-NH_2	21 ± 2[c]	-2

[a]Charge replacement mutations are shown in bold red. Amino acid changes incorporated from earlier peptides are shown in blue. [b]K_d values derived from IC_{50} values measured in an FPA competition assay unless otherwise noted. [c]K_d values determined by direct binding experiments.

negatively charged amino acids is tolerated, other substitutions are accompanied by a severe drop in binding affinity, as might be expected for a peptide binding to a protonated basic cleft. For example, changing D1 to an asparagine was tolerated with a relatively minimal loss of affinity (peptide-21), an alanine substitution of D5 did not reduce the potency compared to an N substitution (peptide-22 and peptide-23), and substitution of D6 with an asparagine produced better binding than the corresponding alanine (peptide-24 and peptide-25). However, for E8, an alanine substitution sharply reduced the binding affinity (peptide-26), while minimal loss of affinity was observed for substituting E9 with either an alanine or glutamine (peptide-27 and peptide-28). On the basis of these results, we combined the least deleterious amino acid substitutions to produce a FITC-labeled peptide (peptide-29) with a net negative charge of −2. However, the reduction in charge came at the expense of a nearly 50-fold loss in binding to RPA70N compared to peptide-20.

Shortening of the Peptide Sequence. Concomitant with our efforts to reduce the net negative charge of the peptides, we examined the effect of peptide length on binding affinity and the possibility of improving the properties of the peptides.[22] If the ATRIP-derived peptides adopt a helix with the same length as p53 upon binding to RPA70N, several N- and the C-terminal residues may not be part of the secondary structure and thus are potential candidates for removal. The alanine scan revealed that all residues at the N-terminus are essential for interacting with RPA70N (Table 1). In contrast, minimal loss of binding affinity was observed when residues at the C-terminus were replaced by alanine (peptide-12 and peptide-13). Therefore, we tested whether shortening of peptide-20 by one, two, or three residues at the C-terminus would be tolerated (Table 4).

Table 4. Binding Affinity of Shortened Peptides

Peptide Name	Amino Acid Sequence[a]	FPA K_d (μM)[b]
Peptide-20	FITC-DFTADDLEEWFALAS-NH_2	0.48 ± 0.03
Peptide-30	FITC-DFTADDLEEWFALA**-**-NH_2	0.58 ± 0.03
Peptide-31	FITC-DFTADDLEEWFAL**--**-NH_2	0.33 ± 0.02
Peptide-32	FITC-DFTADDLEEWFA**---**-NH_2	0.91 ± 0.01
Peptide-33	FITC-DFTADDLEEW**Z**AL**--**-NH_2	0.022 ± 0.005

[a]Deleted residues are indicated by bold red dashes. 3,4-Dichlorophenylalanine is shown as a bold green Z. Amino acid changes incorporated from earlier peptides are shown in blue. [b]K_d values determined by direct binding experiments.

Removing the C-terminal residue (S15) had almost no effect on the binding of peptide-30 to RPA70N, and the removal of the last two C-terminal amino acids (A-S) led to a peptide with improved binding affinity to RPA70N (peptide-31). However, removing one additional residue (L13) resulted in a 3-fold decrease in binding affinity (peptide-32).

Unnatural Amino Acid Substitutions. In order to further improve binding to RPA70N, we explored the possibility of incorporating unnatural amino acids. Such peptides can be difficult and expensive to synthesize and thus must be carefully designed. To identify suitable locations for incorporation of a designed unnatural amino acid, we exploited findings from our small molecule discovery efforts. We have previously reported the use of an NMR-based fragment screen to discover compounds that bind to a hydrophobic pocket near S55,[12] suggesting that this pocket represents an important binding "hot spot" on RPA70N (Figure 1A). Consistent with this finding, that same pocket is occupied by F54 of the WF motif

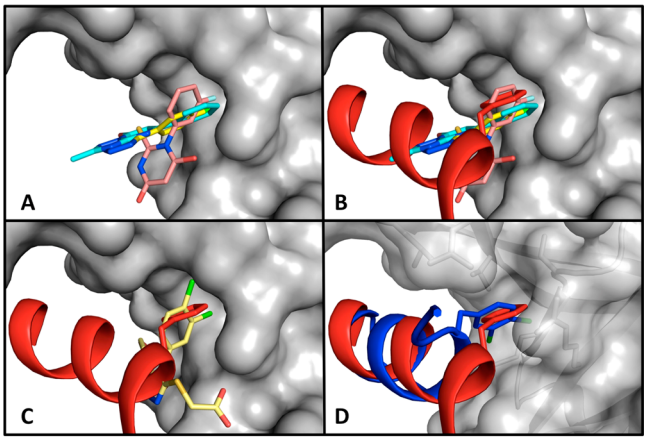

Figure 1. X-ray structures of fragments and peptides in complex with RPA70N reveal a preferred binding site within the basic cleft. (A) Overlay of cocrystal structures of fragments bound to RPA70N. (B) Superpositioned structures of RPA70N bound to fragments and the p53 peptide (red). (C) The dichlorophenyl ring of an elaborated compound (yellow) binds in the same hydrophobic pocket as F54 of the p53 peptide (red). (D) Superposition of RPA70N/p53 peptide (red)[19] and RPA70N/peptide-33 (blue).

dx.doi.org/10.1021/jm401730y | J. Med. Chem. 2014, 57, 2455−2461

within the p53 peptide (Figure 1B).[19] Optimization of multiple series of fragment hits has established that a 3,4-dichloro-substituted phenyl ring displays significantly improved binding affinity to RPA70N compared to an unsubstituted phenyl group.[12,14] Thus, we hypothesized that a peptide containing a 3,4-dichloro-substituted phenylalanine in place of a phenylalanine would have improved binding affinity to RPA70N (Figure 1C). Indeed, a peptide containing an unnatural amino acid with a 3,4-dichlorophenyl moiety (peptide-33) showed a >100-fold improvement in affinity (Table 4). An X-ray structure of peptide-33 when complexed with RPA70N confirmed that the side chain of the 3,4-dichlorophenylalanine binds to the RPA70N hot spot located above S55, in a manner similar to the binding mode of the phenylalanine of p53 (Figure 1D).

Stapled Helix Peptides. The use of a hydrocarbon staple for helical peptides is a promising approach to improve upon the poor characteristics of linear peptides by imparting increased protease resistance, affinity, and cell permeability.[15−17] Three stapling patterns have been shown to stabilize helical conformations: *i*, *i* + 3; *i*, *i* + 4; and *i*, *i* + 7.[17] On the basis of the results from the mutational analyses, we employed the *i*, *i* + 4 configuration using residues 5 and 9 to evaluate stapled helix peptides with varying overall net charge (Table 5).

Table 5. Binding Affinities of Peptides

Name	Amino Acid Sequence[a]	FPA K_d (μM)[b]	Charge
Peptide-31	FITC-DFTADDLEEWFAL---NH_2	0.33 ± 0.02	-6
Peptide-34	FITC-DFTAXDLEXWFAL---NH_2	0.57 ± 0.1	-4
Peptide-35	FITC-NFTAXDLEXWFAL---NH_2	1.5 ± 0.04	-3
Peptide-36	FITC-DFTAXNLEXWFAL---NH_2	3.7 ± 0.7	-3
Peptide-37	FITC-NFTAXNLEXWFAL---NH_2	7.4 ± 0.6	-2
Peptide-38	FITC-NFTAXDLEXWZAL---NH_2	0.048 ± 0.015	-3
Peptide-39	FITC-NFTAXNLEXWZAL---NH_2	0.042 ± 0.012	-2

[a]α-(4-Pentenyl)alanine staples are depicted as a red X. 3,4-Dichlorophenylalanine is shown as a bold green Z. Amino acid changes incorporated from earlier peptides are shown in blue. [b]K_d values determined by direct binding experiments.

Although peptide-34 had a slightly reduced binding affinity compared to its unstapled counterpart (peptide-31), the negative charge was reduced. As expected, further reduction of the charge yielded an additional loss in affinity (peptide-35, peptide-36, and peptide-37). Once again, we compensated for the loss in affinity due to charge abrogation by substituting F12 with a dichlorophenylalanine (peptide-38 and peptide-39). Incorporation of this motif alone led to a 31- and 175-fold increase in affinity, respectively, resulting in peptides that represent the optimal balance of potency and overall net charge.

Selectivity. To verify the utility of the stapled helix peptides as specific inhibitors of the RPA70N protein−protein interactions, we evaluated the ability of the peptides to bind to the other OB-fold-containing domains of RPA that bind to ssDNA.

By use of a direct binding FPA assay, peptide-37 and peptide-39 were examined for their ability to bind to RPA70A/B, which contains the core ssDNA binding unit, and RPA70C/32D/14 (Figure 2). Peptide-37 shows very little selectivity in binding to the different OB-fold containing domains; while this peptide binds to RPA70N with a K_d of 7.4 μM, it binds the other domains with similar affinity (12−15 μM). In contrast, peptide-39, which binds to RPA70N with an affinity of 0.042 μM, binds to RPA70A/B and RPA70C/32D/14 with a K_d of only 2.4 μM, exhibiting 50-fold selectivity for binding to RPA70N. The incorporation of the dichlorophenyl moiety not only produces a significant increase in potency but also appears to impart a significant increase in selectivity for RPA70N over other OB-fold containing domains. To confirm that peptide-39 does not functionally displace RPA from ssDNA, we conducted an electrophoretic mobility shift assay (EMSA). Increasing concentrations of peptide-39 were incubated with RPA and ssDNA and subjected to separation on a polyacrylamide gel. No change in the percent of RPA bound to radiolabeled ssDNA was observed, indicating that although peptide-39 can bind weakly to other OB-fold containing domains in a biochemical assay, this 2 μM binding affinity is not sufficient to displace full-length RPA from ssDNA (Figure 3). Thus, peptide-39 possesses a suitable selectivity profile for use as a probe of RPA70N function in cells.

Cell Penetrance. Several studies have demonstrated that stapled helix peptides gain entry to mammalian cells through active endocytosis.[15,23,24] Further, overall peptide charge is a key determinant of cellular penetrance, with increased positive charge leading to more efficient uptake. We examined the ATRIP-derived stapled helix peptides for their ability to enter mammalian cells. Peptides were incubated for 24 h with U2OS cells, fixed, and visualized by confocal microscopy for direct observation of the FITC label (Figure 4). As expected, peptide-34, with a net charge of −4, was the least efficient at penetrating cells. In contrast, the remaining peptides were observed inside

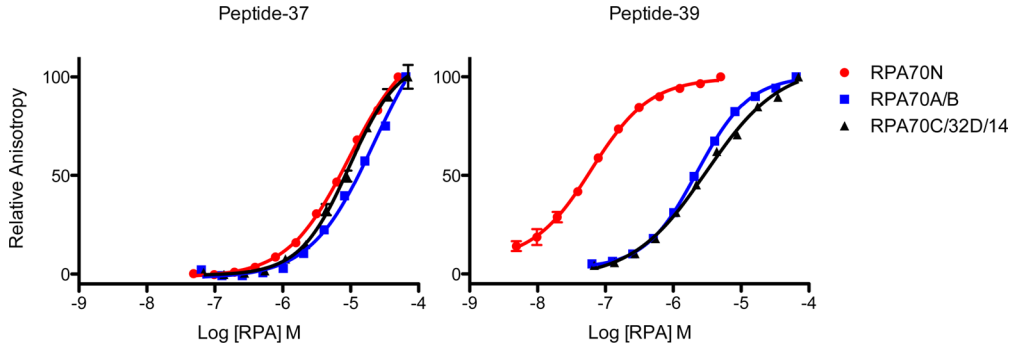

Figure 2. Peptide-39 is selective for binding to RPA70N. Peptide-37 and peptide-39 were incubated with increasing concentrations of the indicated RPA70 constructs. Because of the different sizes of the protein constructs used, data are normalized to the maximal anisotropy for each construct.

dx.doi.org/10.1021/jm401730y | J. Med. Chem. 2014, 57, 2455−2461

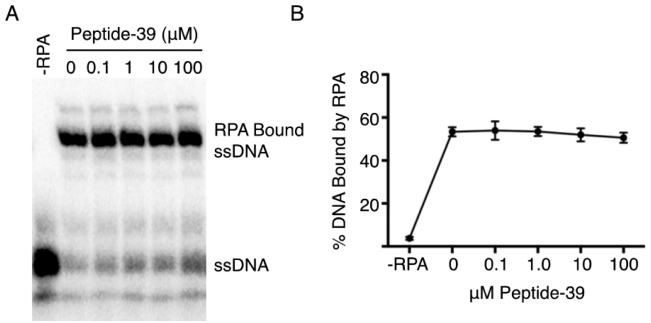

Figure 3. Peptide-39 does not displace RPA from ssDNA. (A) RPA and ssDNA were incubated with increasing concentrations of peptide-39 prior to separation on a polyacrylamide gel. (B) Quantification of three replicates.

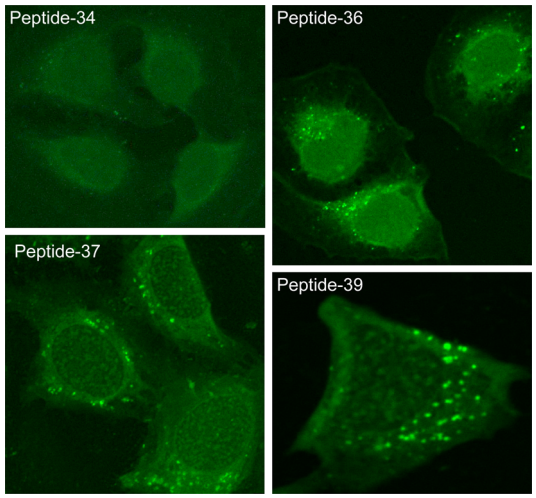

Figure 4. FITC-labeled stapled helix peptides are visible within U2OS cells.

the cells in a pattern consistent with internalization through endocytosis. Diffuse cytosolic staining and fluorescence within the nucleus were also observed, as exemplified by peptide-37 and peptide-39.

CONCLUSIONS

To discover a peptide that binds tightly to RPA70N and penetrates cells, we initiated optimization of a 15 amino acid ATRIP-derived peptide that binds to RPA70N with an affinity of 29 μM and possesses a net charge of −5. Through alanine scanning, natural amino acid substitutions, and shortening of the peptide sequence, we identified key residues responsible for binding to RPA70N, improved the binding affinity, and ascertained which amino acids could be substituted to reduce the overall negative charge. However, because of the electrostatic characteristics of the pocket, substitutions that reduced the peptide charge universally led to a decrease in binding affinity. Despite these improvements and the knowledge gained, the resulting peptides were still unsuitable for use as a chemical probe for the study of RPA70N as a cancer target because of insufficient binding affinity.

To further improve the binding affinity, we sought to incorporate an unnatural amino acid into our peptides. Historically, this strategy has not been widely employed because of difficulties in choosing which amino acid to replace and which unnatural amino acid to use as a replacement. Indeed, most peptide optimizations typically involve only the use of natural amino acid substitutions. Here we have demonstrated a strategy to efficiently design unnatural amino acid substitutions for peptide optimization. The optimization process involves the identification of a binding hot spot using a fragment-based screen and subsequent structural characterization of important molecular interactions that might be exploited for affinity improvements. Structural knowledge of the residue that normally occupies this hotspot, along with SAR information gleaned from fragment hits and optimization of these hits, then guides the efficient targeted replacement of an amino acid with an optimized variant.

We have demonstrated this strategy by capitalizing on a wealth of SAR and structural information from compounds identified from a NMR-based fragment screen. In multiple prior instances, the presence of a 3,4-dichlorophenyl moiety has produced improvements in binding affinity.[12,14] Thus, we applied this substitution pattern to a phenylalanine residue that had been previously determined to occupy the same binding hot spot identified in the fragment screen. The addition of two halogens produced highly significant gains in binding affinity in both stapled and unstapled peptides.

In total, by combining peptide optimization studies, small molecule SAR, and structural information on peptide and small molecule binding modes, we improved the affinity of the modified peptide by almost 1000-fold. The optimized stapled helix peptide obtained from this work binds tightly to RPA70N with an affinity of 0.042 μM, is selective for binding to RPA70N versus other OB folds of RPA, has a reduced overall net negative charge, and penetrates cells. This compound may serve as a useful tool to study the biology of RPA and validate RPA as a cancer target. Moreover, the new approach that we have employed to optimize the peptides may be a useful general method for optimizing peptides that bind to other protein targets and thus expand the utility of stapled helix peptides as chemical tools and therapeutic agents.

EXPERIMENTAL DETAILS

Protein Expression and Purification. Recombinant RPA70N ($RPA70_{1-120}$), RPA70AB ($RPA70_{181-422}$), and RPA70NAB ($RPA70_{1-422}$) constructs were prepared as described previously.[20,25−27] Proteins were expressed in *Escherichia coli* host Rosetta (RPA70AB, RPA70NAB) or BL21-DE3 (RPA70N) cells (Novagen). Cells were grown in LB medium containing kanamycin (RPA70AB, RPA70NAB) or ampicillin (RPA70N) at 37 °C, induced with 0.1 M IPTG when the OD reached 0.6, and harvested after 4 h using a JLA 8.1 Beckman rotor at 7500 rpm and 4 °C. Pellets were stored at −20 °C. Human RPA70N was purified using a Ni sepharose column (GE Healthcare). Following His-tag cleavage and a Ni sepharose column repass to remove the cleaved tag, RPA70N was obtained at greater than 95% purity as judged by sodium dodecyl sulfate−polyacrylamide gel electrophoresis (SDS−PAGE) analysis. Finally, RPA70N samples were dialyzed against assay buffer (50 mM HEPES, 75 mM NaCl, 5 mM DTT, pH 7.5) for use in fluorescence polarization studies. RPA70AB samples were purified using nickel affinity chromatography in 10 mM HEPES (pH 7.5), 500 mM NaCl, 5 mM BME, and 10% glycerol using an elution gradient from 20 to 300 mM imidazole. Cleavage of the His tag with TEV protease was performed through overnight dialysis in a buffer containing 10 mM HEPES (pH 7.5), 200 mM NaCl, 5 mM BME. A second Ni column purification step was used to remove the His tag. Size exclusion chromatography using a Superdex S75 column equilibrated with the dialysis buffer was used as a last step of purification. RPA70AB protein was concentrated, and stock solutions were frozen in liquid nitrogen and kept at −80 °C. A similar procedure described previously[26] was used for RPA70NAB

dx.doi.org/10.1021/jm401730y | J. Med. Chem. 2014, 57, 2455−2461

samples using Ni column buffer 30 mM MES (pH 6.5), 500 mM NaCl, 5 mM BME and cleaving with H3C protease. The size exclusion chromotography step was performed using a Superdex S200 column and a buffer containing 30 mM MES (pH 6.5), 200 mM NaCl, 10 mM BME, 5% glycerol.

Peptide Synthesis. All linear peptides, with and without fluorescein isothiocyanate (FITC), were purchased from GenScript USA Inc. FITC groups were attached to the N-terminus of peptide sequences via an aminohexanoic acid (Ahx) linker. Hydrocarbon stapled peptides were purchased from New England Peptide LLC. Staples were incorporated by placing modified α-(4-pentenyl)alanine residues at predetermined locations within the peptide sequence, separated by three amino acids. Peptides were purified by the manufacturer using high-performance liquid chromatography to >95% purity. Unlabeled peptides were dissolved as 10 mM stock solutions in assay buffer (50 mM HEPES, 75 mM NaCl, 5 mM DTT, pH 7.5). FITC-labeled peptides were dissolved in DMSO to a final concentration of 1 mM.

Fluorescence Polarization Anisotropy Assays. K_d determination and FPA competition assays were conducted as described previously[20] with minor modifications. For direct K_d determination of FITC-labeled peptides, increasing concentrations of purified RPA were added to 25 nM peptide in a total of 50 μL assay buffer. Anisotropy was measured, and data were fit to a single site binding model using Prism. For competition experiments, unlabeled peptides were titrated into assay buffer containing RPA70N and FITC-labeled peptide probe. Assays were conducted at a protein concentration equal to the K_d of the FITC-peptide−protein interaction. Therefore, 50 nM FITC-ATRIP was used with 6 μM RPA70N; 25 nM peptide-31 was used with 350 nM RPA70N. Anisotropy was measured and plotted against compound concentration using a four-parameter logistic fit to generate an IC_{50}; this value was converted to K_d, as previously described.[20]

Gel Mobility Shift Assay. The gel mobility shift assays were performed as previously described[28] with the following modifications. Purified RPA (12 nM final concentration) and increasing concentrations of peptide-39 (0, 0.1, 1, 10, 100 μM final concentration) were incubated with radiolabeled 50-nucleotide ssDNA probe (6 nM final concentration) at room temperature for 20 min. The samples were separated by electrophoresis prior to autoradiography and quantitation.

Fluorescence Microscopy. U2OS cells were plated at 3×10^4 cells/well in eight-chamber slides (BD Falcon). After 24 h, cells were washed once with PBS and incubated for 24 h with stapled helix peptides in serum-free medium. Medium was removed, and cells were fixed in 4% paraformaldehyde/PBS for 1 h at room temperature. Cells were rinsed three times with PBS and mounted on a coverslip with Vectashield (Vector Laboratories) mounting medium containing DAPI. Slides were imaged on a confocal microscope (Zeiss LSM 710).

Crystallization of RPA70N:Peptide-33 Complex. Lyophilized peptide-33 (FITC-Ahx-DFTADDLEEWZAL-NH_2) was added directly to 700 μM RPA70N E7R at a 2.5:1 (peptide-33/E7R RPA70N) ratio and initially screened against a variety of conditions. Following optimization of the initial crystallization conditions, the buffer condition of 100 mM Bis-Tris, pH 6.5, 200 mM ammonium acetate, 25% PEG 3350 was found to produce crystals that showed a strong green color, indicative of the presence of FITC. Prior to data collection, crystals were soaked in mother liquor containing 20% 2-methyl-2,4-pentanediol (MPD) and were flash-frozen in liquid nitrogen. X-ray diffraction data were initially collected on an in-house rotating anode source and later at sector 21 (Life Sciences Collaborative Access Team, LSCAT) at the Advanced Photon Source. All data were processed by HKL2000.[29] The proteins crystallized in space group C121 and contained two peptide-33:E7R RPA70N complexes in the asymmetric unit. Initial phases were obtained by molecular replacement with PHASER[30] using the E7R RPA70N structure (4IPC)[27] as a search model. Iterative cycles of model building and refinement were performed using COOT[31] and Phenix.[32] Following modeling of waters, peptide-33, including its covalently attached FITC, was placed into electron density at the basic cleft and refined. The structure of this complex has been deposited in the Protein Data Bank under the accession code 4NB3.

■ ASSOCIATED CONTENT

Ⓢ Supporting Information

Crystallographic results and refinement statistics. This material is available free of charge via the Internet at http://pubs.acs.org.

Accession Codes

The structures of compounds bound to E7R have been deposited in the Protein Data Bank under accession code 4NB3.

■ AUTHOR INFORMATION

Corresponding Author

*Phone: 615-322-6303. E-mail: stephen.fesik@vanderbilt.edu.

Present Addresses

[#]A.O.F.: Novartis Institutes for BioMedical Research (NIBR), Global Discovery Chemistry, Emeryville, California 94608, United States.

[∞]B.V.: The Institute for Applied Cancer Sciences, The University of Texas MD Anderson Cancer Center, Houston, TX, United States.

[¶]E.M.S.-F.: Physiology and Biophysics Department, Federal University of Minas Gerais, Av. Antônio Carlos, 6627, Pampulha, Belo Horizonte, MG, 31270-901, Brazil.

Notes

The authors declare no competing financial interest.

■ ACKNOWLEDGMENTS

This work was supported by a postdoctoral fellowship from the Deutscher Akademischer Austausch Dienst (DAAD) to A.O.F., a National Institutes of Health National Research Service Award (NRSA) F32 ES021690 to M.D.F., NIH Grant CA102792 to D.C., and funding from the National Council for Scientific and Technological Development—CNPq and Federal University of Minas Gerais/Brazil to E.M.S.-F. We thank Dr. Cheryl Arrowsmith (Ontario Cancer Institute, Toronto, Canada) for kindly providing the ^1H and ^{15}N backbone NMR assignments of RPA70N.

■ ABBREVIATIONS USED

RPA, replication protein A; FPA, fluorescence polarization anisotropy; LE, ligand efficiency

■ REFERENCES

(1) Wold, M. S. Replication protein A: a heterotrimeric, single-stranded DNA-binding protein required for eukaryotic DNA metabolism. *Annu. Rev. Biochem.* **1997**, *66*, 61−92.

(2) Fanning, E.; Klimovich, V.; Nager, A. R. A dynamic model for replication protein A (RPA) function in DNA processing pathways. *Nucleic Acids Res.* **2006**, *34*, 4126−4137.

(3) Majka, J.; Binz, S. K.; Wold, M. S.; Burgers, P. M. Replication protein A directs loading of the DNA damage checkpoint clamp to 5′-DNA junctions. *J. Biol. Chem.* **2006**, *281*, 27855−27861.

(4) Cortez, D.; Guntuku, S.; Qin, J.; Elledge, S. J. ATR and ATRIP: partners in checkpoint signaling. *Science* **2001**, *294*, 1713−1716.

(5) Bartkova, J.; Horejsi, Z.; Koed, K.; Kramer, A.; Tort, F.; Zieger, K.; Guldberg, P.; Sehested, M.; Nesland, J. M.; Lukas, C.; Orntoft, T.; Lukas, J.; Bartek, J. DNA damage response as a candidate anti-cancer barrier in early human tumorigenesis. *Nature* **2005**, *434*, 864−870.

(6) Theobald, D. L.; Mitton-Fry, R. M.; Wuttke, D. S. Nucleic acid recognition by OB-fold proteins. *Annu. Rev. Biophys. Biomol. Struct.* **2003**, *32*, 115−133.

(7) Stauffer, M. E.; Chazin, W. J. Physical interaction between replication protein A and Rad51 promotes exchange on single-stranded DNA. *J. Biol. Chem.* **2004**, *279*, 25638−25645.
(8) Bochkarev, A.; Bochkareva, E. From RPA to BRCA2: lessons from single-stranded DNA binding by the OB-fold. *Curr. Opin. Struct. Biol.* **2004**, *14*, 36−42.
(9) Zou, L.; Elledge, S. J. Sensing DNA damage through ATRIP recognition of RPA-ssDNA complexes. *Science* **2003**, *300*, 1542−1548.
(10) Shechter, D.; Costanzo, V.; Gautier, J. ATR and ATM regulate the timing of DNA replication origin firing. *Nat. Cell Biol.* **2004**, *6*, 648−655.
(11) Ball, H. L.; Myers, J. S.; Cortez, D. ATRIP binding to replication protein A-single-stranded DNA promotes ATR-ATRIP localization but is dispensable for Chk1 phosphorylation. *Mol. Biol. Cell* **2005**, *16*, 2372−2381.
(12) Frank, A. O.; Feldkamp, M. D.; Kennedy, J. P.; Waterson, A. G.; Pelz, N. F.; Patrone, J. D.; Vangamudi, B.; Camper, D. V.; Rossanese, O. W.; Chazin, W. J.; Fesik, S. W. Discovery of a potent inhibitor of replication protein A protein−protein interactions using a fragment linking approach. *J. Med. Chem.* **2013**, *56*, 9242−9250.
(13) Glanzer, J. G.; Liu, S. Q.; Oakley, G. G. Small molecule inhibitor of the RPA70 N-terminal protein interaction domain discovered using in silico and in vitro methods. *Bioorg. Med. Chem.* **2011**, *19*, 2589−2595.
(14) Patrone, J. D.; Kennedy, J. P.; Frank, A. O.; Feldkamp, M. D.; Vangamudi, B.; Pelz, N. F.; Rossanese, O. W.; Waterson, A. G.; Chazin, W. J.; Fesik, S. W. Discovery of protein−protein interaction inhibitors of replication protein A. *ACS Med. Chem. Lett.* **2013**, *4*, 601−605.
(15) Walensky, L. D.; Kung, A. L.; Escher, I.; Malia, T. J.; Barbuto, S.; Wright, R. D.; Wagner, G.; Verdine, G. L.; Korsmeyer, S. J. Activation of apoptosis in vivo by a hydrocarbon-stapled BH3 helix. *Science* **2004**, *305*, 1466−1470.
(16) Walensky, L. D.; Pitter, K.; Morash, J.; Oh, K. J.; Barbuto, S.; Fisher, J.; Smith, E.; Verdine, G. L.; Korsmeyer, S. J. A stapled BID BH3 helix directly binds and activates BAX. *Mol. Cell* **2006**, *24*, 199−210.
(17) Verdine, G. L.; Hilinski, G. J. Stapled peptides for intracellular drug targets. *Methods Enzymol.* **2012**, *503*, 3−33.
(18) Xu, X.; Vaithiyalingam, S.; Glick, G. G.; Mordes, D. A.; Chazin, W. J.; Cortez, D. The basic cleft of RPA70N binds multiple checkpoint proteins, including RAD9, to regulate ATR signaling. *Mol. Cell. Biol.* **2008**, *28*, 7345−7353.
(19) Bochkareva, E.; Kaustov, L.; Ayed, A.; Yi, G. S.; Lu, Y.; Pineda-Lucena, A.; Liao, J. C.; Okorokov, A. L.; Milner, J.; Arrowsmith, C. H.; Bochkarev, A. Single-stranded DNA mimicry in the p53 transactivation domain interaction with replication protein A. *Proc. Natl Acad. Sci. U.S.A.* **2005**, *102*, 15412−15417.
(20) Souza-Fagundes, E. M.; Frank, A. O.; Feldkamp, M. D.; Dorset, D. C.; Chazin, W. J.; Rossanese, O. W.; Olejniczak, E. T.; Fesik, S. W. A high-throughput fluorescence polarization anisotropy assay for the 70N domain of replication protein A. *Anal. Biochem.* **2012**, *421*, 742−749.
(21) Morin, G.; Fradet-Turcotte, A.; Di Lello, P.; Bergeron-Labrecque, F.; Omichinski, J. G.; Archambault, J. A conserved amphipathic helix in the N-terminal regulatory region of the papillomavirus E1 helicase is required for efficient viral DNA replication. *J. Virol.* **2011**, *85*, 5287−5300.
(22) Demmer, O.; Frank, A. O.; Kessler, H. Design of Cyclic Peptides. In *Peptide and Protein Design for Biopharmaceutical Applications*; Jensen, K. J., Ed.; Wiley: Hoboken, NJ, 2009; Chapter 4, p xii, 294 pp, 296 pp of plates.
(23) Bernal, F.; Tyler, A. F.; Korsmeyer, S. J.; Walensky, L. D.; Verdine, G. L. Reactivation of the p53 tumor suppressor pathway by a stapled p53 peptide. *J. Am. Chem. Soc.* **2007**, *129*, 2456−2457.
(24) Moellering, R. E.; Cornejo, M.; Davis, T. N.; Del Bianco, C.; Aster, J. C.; Blacklow, S. C.; Kung, A. L.; Gilliland, D. G.; Verdine, G. L.; Bradner, J. E. Direct inhibition of the NOTCH transcription factor complex. *Nature* **2009**, *462*, 182−188.
(25) Arunkumar, A. I.; Stauffer, M. E.; Bochkareva, E.; Bochkarev, A.; Chazin, W. J. Independent and coordinated functions of replication protein A tandem high affinity single-stranded DNA binding domains. *J. Biol. Chem.* **2003**, *278*, 41077−41082.
(26) Brosey, C. A.; Chagot, M. E.; Ehrhardt, M.; Pretto, D. I.; Weiner, B. E.; Chazin, W. J. NMR analysis of the architecture and functional remodeling of a modular multidomain protein, RPA. *J. Am. Chem. Soc.* **2009**, *131*, 6346−6347.
(27) Feldkamp, M. D.; Frank, A. O.; Kennedy, J. P.; Patrone, J. D.; Vangamudi, B.; Waterson, A. G.; Fesik, S. W.; Chazin, W. J. Surface reengineering of RPA70N enables cocrystallization with an inhibitor of the replication protein A interaction motif of ATR interacting protein. *Biochemistry* **2013**, *52*, 6515−6524.
(28) Betous, R.; Mason, A. C.; Rambo, R. P.; Bansbach, C. E.; Badu-Nkansah, A.; Sirbu, B. M.; Eichman, B. F.; Cortez, D. SMARCAL1 catalyzes fork regression and Holliday junction migration to maintain genome stability during DNA replication. *Genes Dev.* **2012**, *26*, 151−162.
(29) Otwinowski, Z.; Minor, W. Processing of X-ray Diffraction Data Collected in Oscillation Mode. In *Macromolecular Crystallography. Part A*; Carter, C. W., Jr., Sweet, R. M., Eds.; Academic Press: San Diego, CA, 1997; Vol. *276*, pp 307−326.
(30) McCoy, A. J.; Grosse-Kunstleve, R. W.; Adams, P. D.; Winn, M. D.; Storoni, L. C.; Read, R. J. Phaser crystallographic software. *J. Appl. Crystallogr.* **2007**, *40*, 658−674.
(31) Emsley, P.; Cowtan, K. Coot: model-building tools for molecular graphics. *Acta Crystallogr., Sect. D: Biol. Crystallogr.* **2004**, *60*, 2126−2132.
(32) Adams, P. D.; Grosse-Kunstleve, R. W.; Hung, L. W.; Ioerger, T. R.; McCoy, A. J.; Moriarty, N. W.; Read, R. J.; Sacchettini, J. C.; Sauter, N. K.; Terwilliger, T. C. PHENIX: building new software for automated crystallographic structure determination. *Acta Crystallogr., Sect. D: Biol. Crystallogr.* **2002**, *58*, 1948−1954.